Wildlife Society Bulletin 43(4):619–629; 2019; DOI: 10.1002/wsb.1018

Original Article

Predicting Forest Understory Habitat for Canada Lynx Using LIDAR Data

PATRICK A. FEKETY,[1] *Department of Ecosystem Science & Sustainability, Colorado State University, Campus Delivery 1476, Fort Collins, CO 80523, USA*

REMA B. SADAK, *U.S. Department of Agriculture Forest Service, Intermountain Region, 324 25th Street, Ogden, UT 84401, USA*

JOEL D. SAUDER, *Idaho Department of Fish and Game, 3316 16th Street, Lewiston, ID 83501, USA*

ANDREW T. HUDAK, *U.S. Department of Agriculture Forest Service, Rocky Mountain Research Station, 1221 S Main Street, Moscow ID 83843, USA*

MICHAEL J. FALKOWSKI, *Department of Ecosystem Science & Sustainability, Colorado State University, Campus Delivery 1476, Fort Collins, CO 80523, USA*

ABSTRACT Canada lynx (*Lynx canadensis*) is a federally threatened species in the contiguous United States. Within National Forests covered by the Northern Rockies Lynx Management Direction, Federal land managers must consider the effect of management activities on Canada lynx habitat. A common method to assess Canada lynx habitat used by the U.S. Forest Service is to measure horizontal cover using a cover board. We used field measurements and airborne Light Detection and Ranging (LIDAR) metrics to test beta regression models that predict estimates of horizontal cover on the Nez Perce–Clearwater National Forest, Idaho, USA, 2009–2015. We also investigated the effect on model predictions when the cover board was blocked by the main stem of a tree. Model fit statistics for normalized root mean square errors (RMSE%) were 30.8–33.7% and pseudo-R^2 ranged from 0.64 to 0.71. Using independent validation data, model performance statistics for RMSE% were 24.6–33.5% and R^2 ranged from 0.51 to 0.69. We found that removing cover board measurements where the main stem of a tree blocked >75% of the cover board produced the best model statistics. These models can be applied across LIDAR extents resulting in maps of horizontal cover estimates, which may be used in assessing effects of management activities on Canada lynx habitat.

KEY WORDS beta regression, cover board, horizontal cover, *Lynx canadensis*, Northern Rocky Mountains.

Forest understories provide essential resources to numerous wildlife species and are an important component in wildlife habitat management. Understories provide hiding cover for both predators and prey, a source of food, and thermal protection (Moreno et al. 1996, Mysterud and Ostbye 1999, Hagar 2007). Identifying and managing understory attributes are important considerations in managing wildlife habitat (Smith and Long 1987, Martinuzzi et al. 2009). For example, snowshoe hares (*Lepus americanus*) use dense understories as a food source and for cover and security from predators; consequently, dense horizontal cover is an important determinant of snowshoe hare presence and abundance (Hodges et al. 2009, Lewis et al. 2011, Berg et al. 2012, Ivan et al. 2014, Holbrook et al. 2017). Canada lynx (*Lynx canadensis*) predominantly prey on snowshoe hares; therefore, many management decisions made by the U.S. Forest Service (USFS) focus on providing and maintaining snowshoe hare habitat (Elton and Nicholson 1942, Ruggiero et al. 1999).

In the United States, the Canada lynx was designated federally threatened in 14 states based on inadequate regulatory mechanisms to conserve the species in federal land management plans (U.S. Fish and Wildlife Service 2000). Protection was extended to Canada lynx in the contiguous United States in 2014 (U.S. Fish and Wildlife Service 2014). In the Rocky Mountains, >75% of the critical Canada lynx habitat, as defined by the U.S. Fish and Wildlife Service, is on land managed by the USFS. In March 2007, 18 National Forest Plans were amended with the Northern Rockies Lynx Management Direction (NRLMD) Record of Decision, with the goal being to provide specific management direction in project planning and implementation designed to conserve Canada lynx and its habitat (USDA Forest Service 2007). Standards and guidelines for the conservation of Canada lynx and snowshoe hare are incorporated in the NRLMD, to ensure that the USFS will plan projects within Canada lynx habitat in ways that either benefit or avoid long-term adverse effects to the species or its habitat.

Received: 19 November 2018; Accepted: 27 June 2019
Published: 7 November 2019

[1]*E-mail: patrick.fekety@colostate.edu*

Habitat suitability for Canada lynx on USFS land must be determined within a proposed project area prior to project implementation. In the Rocky Mountains, winter Canada lynx habitat is limited and thus guides management decisions. Prior to conducting vegetation management activities in Canada lynx habitat within lynx analysis units, assessment of horizontal cover at the project level is necessary to determine if the forest stands proposed for treatment are likely to provide foraging habitat for snowshoe hare, and thus provide Canada lynx habitat. The NRLMD has standards that limit vegetation management activities from reducing winter snowshoe hare habitat by prohibiting most vegetation management in multistoried mature and late successional forests (USDA Forest Service 2007). Standards also exist that prohibit precommercial thinning in forests in the stand initiation structural stage in Canada lynx habitat within lynx analysis units (USDA Forest Service 2007).

A horizontal cover assessment is conducted to determine whether multistory stands provide winter snowshoe hare cover above a threshold value; however, it is not necessary that the stands be measured in winter. If, in multistory stands, the horizontal cover is ≥35% of measured horizontal cover in winter surveys or 48% in summer surveys, then the forest stands are considered winter hare foraging habitat and, with a few exceptions, vegetation management is prohibited in these multistoried stands (USDA Forest Service 2007, Bertram and Claar 2009). Typically, these cover assessments are done with on-the-ground surveys using cover boards.

Cover boards (Nudds 1977) are routinely used to measure the horizontal component of a forest understory and have been used to assess Canada lynx (Squires et al. 2008) and snowshoe hare (Hodges et al. 2009) habitat in addition to other species (e.g., Jones 1968). In the Rocky Mountains, cover boards used in hare or lynx studies typically measure 0.5 m × 2.0 m and are placed at 5–11.2 m distances from the observer (Squires et al. 2008, 2010; Cheng et al. 2010; Hodson et al. 2012). The proportion of cover board obscured is either visually assessed in the field or in the laboratory from photographs. The agent causing the obstruction is not considered when assessing horizontal cover. To obtain plot-level estimates, multiple observations are taken, facing prespecified directions, and horizontal cover is averaged across the plot. Prespecifying directions reduces observation bias, but does not guarantee that the observations are representative of the plot. Additionally, the plot-based nature of cover board measurements limits the spatial area where sampling realistically can occur.

Predictive modeling employing remote-sensing products may extend horizontal cover estimates to spatial extents larger than what can be visited in the field to conduct cover board measurements. Airborne LIDAR (Light Detection and Ranging) might be well-suited to assist in predicting horizontal cover estimates (Kramer et al. 2016, Campbell et al. 2018). Light Detection and Ranging is an active remote-sensing technology that uses a laser to accurately sample the 3-dimensional structure of a forest. An aircraft equipped with a LIDAR unit emits a laser pulse toward the ground and the laser reflection is returned to a sensor on the aircraft. The time-of-flight of the laser pulse, a global navigation satellite system (GNSS; e.g., Global Positioning System), and inertial measurement unit (which measures aircraft orientation) work in tandem to accurately calculate the position of the object causing the laser reflection. Light Detection and Ranging returns are classified to determine what caused the reflection—for example, ground, vegetation, or unknown (ASPRS 2013). Classified LIDAR returns are used to produce maps representing topography and various forest structure attributes. Products derived from LIDAR products have been used in many aspects of natural resource management, such as wildlife management (Goetz et al. 2007), hydrology (Schmugge et al. 2002), and forest management (Dubayah and Drake 2000, Næsset 2002).

Use of LIDAR is appropriate to assist in modeling horizontal cover because both LIDAR and cover boards permit measurement of obstructions. Cover boards enable measurements of obstructions in 2 dimensions (height and width) at a specified distance from an observer, whereas LIDAR measures the location of obstructions in x-, y-, and z-coordinates that characterize the 3-dimensional structure of the forest understory. Cover boards facilitate horizontal cover measurements at specific locations (i.e., field plots), whereas LIDAR is advantageous because it provides 3-dimensional data at high spatial resolutions across large spatial extents.

Resource management occurs at many spatial scales, from the stand-level to the forest-level, and having horizontal cover estimates across large spatial extents could allow resource managers to make more informed decisions regarding both wildlife and vegetation management activities. Our goal was to create and evaluate a LIDAR-based model to estimate horizontal vegetation cover across large spatial extents that could ultimately be used in wildlife habitat management, with a specific focus on aiding the management of the federally listed Canada lynx. Because the placement of the cover board within a plot is typically predetermined and not necessarily representative of the plot conditions, we additionally tested to what extent tree boles obscuring the cover board negatively affect model performance.

STUDY AREA

This study was located on a portion of the Nez Perce–Clearwater National Forests (NPCNF) in Idaho, USA (Fig. 1). The NPCNF was classified as secondary Canada lynx habitat and management activities were required to consider possible effects on Canada lynx or its habitat as required by the Endangered Species Act of 1973 (U.S. Endangered Species Act of 1973, as amended), and consistent with the NRLMD. As of 2016, the NPCNF contracted LIDAR acquisitions for >482,000 ha, which allowed for the testing of predictive modeling approaches

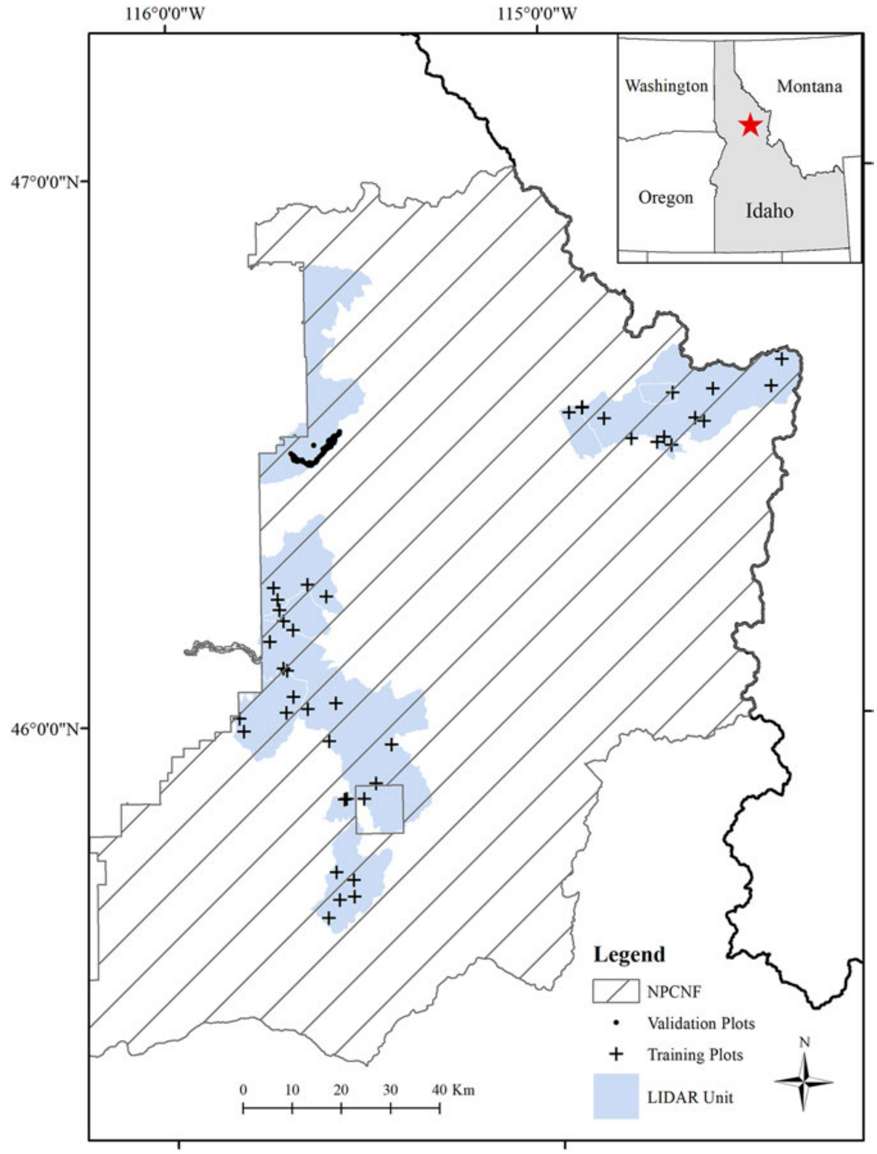

Figure 1. Study area depicting the Nez Perce–Clearwater National Forest, Idaho, USA, and sample locations where understory horizontal-cover models were developed using cover board and Light Detection and Ranging (LIDAR) data for the period 2009–2015.

for characterizing horizontal understory cover. The study area was part of the Bitterroot Range of the Rocky Mountains. Elevation ranged between 450 and 2,500 m. The forest type was classified as mixed conifer primarily composed of Douglas-fir (*Pseudotsuga menziesii*), grand fir (*Abies grandis*), and western redcedar (*Thuja plicata*) with lesser components of ponderosa pine (*Pinus ponderosa*), western larch (*Larix occidentalis*), Engelmann spruce (*Picea engelmannii*), and mountain hemlock (*Tsuga heterophylla*). Bracken fern (*Pteridium aquilinum*) and deciduous shrubs were a major contributor to understory density; major shrub species included alder (*Alnus* spp.), Rocky Mountain maple (*Acer glabrum*), rusty menziesia (*Menziesia ferruginea*), oceanspray (*Holodiscus discolor*), and common snowberry (*Symphoricarpos albus*). The average annual precipitation was approximately 77.9 cm with snow dominating between November and March. Winter minimum temperatures were −11.8° C while summer maximum temperatures were 27.9° C (NOAA 2019).

METHODS

Cover Board Data

We used a cover board that consisted of a checkered pattern of red and white squares, each measuring 0.25 m × 0.25 m. The overall dimensions of the cover board were 0.5 m wide × 2.0 m tall (Fig. 2). Standing at plot center, we took digital photographs of a cover board placed at the edge of the plot. We chose a plot size of 0.04 ha (radius = 11.3 m) because this is the typical forest inventory plot size for the region (USDA Forest Service 2018). We took 4 photographs of the cover board per plot, one facing each cardinal direction. We scored these photographs by estimating the percentage of cover board obscured at 0.5-m height

Figure 2. Examples of cover board digital photographs collected for horizontal cover assessment, Nez Perce–Clearwater National Forest, Idaho, USA, 2015. The cover board was 11.3 m from the observer and each checkered square measured 0.25 m × 0.25 m. (A) Low cover (plot E01 North), (B) medium cover (plot 09A West), (C) dense cover (plot 05A South), and (D) tree bole blocking the cover board (cover board is to the field technician's left; plot 02R East).

increments (4 estimates/photo) and recorded as the midpoint of a 10% cover class (modified from Nudds 1977). We averaged these cover board values from the 4 cardinal directions to obtain plot-level horizontal-cover estimates. Additionally, we also recorded the item causing the obstruction as 1 of 5 classes (tree bole, branches, shrubs, mixture, and other). To assess the influence of tree boles on model results, we subsequently excluded photos when a tree bole blocked >75%, 50%, and 25% of the cover board.

We collected cover board measurements from 41 fixed-area plots in the summer of 2015 for model construction. The temperature while these data were being collected ranged between 15.6° C and 31.1° C and the study area received an average of 3.2 cm of rain. We assigned plots following a stratified random sampling design that crossed 3 levels of elevation, 3 levels of transformed aspect (Roberts and Cooper 1989), and 3 levels of LIDAR-derived mean canopy height. Sampling in this manner helped ensure that plots were placed across a full range of biophysical conditions influencing forest type and structure. Accurate plot locations are needed when combining field measurements and LIDAR data; therefore, we geolocated all plots using a Trimble TRx (Trimble, Sunnyvale, CA, USA) GNSS receiver and differentially corrected to an average horizontal precision <1 m.

An additional 161 cover board plot measurements from a preexisting data set were available for use in this study. These plots measured 0.03 ha (10.0-m radius) and were established in 2014 along a systematic grid with the intent to assess Canada lynx habitat in a planned forest management project area. The field crew geolocated these plots using a Trimble GNSS receiver that did not allow for differential correction. Trimble reported the accuracy of these receivers was typically 1–3 m depending on canopy conditions and GNSS satellite configuration; these accuracies were less than ideal for being used as training data in a LIDAR-derived model; therefore, we reserved them for model validation. The temperature while these data were being collected ranged between 13.3° C and 29.4° C and the study area received an average of 1.8 cm of rain during the period when the coverboard data were collected.

Light Detection and Ranging Data Collection

The NPCNF collected LIDAR for operational management; the cover board plots used as training data were located in 8 separate LIDAR acquisitions and validation data were from a ninth acquisition (Table 1). Local weather records show the temperatures ranged from −2.8° C to 33.9° C on the dates these LIDAR data were collected. A few weather stations recorded small amounts of rain (<1 cm) during this period; however, LIDAR contracts generally prohibit data collection during or immediately after rain events.

To prepare the raw LIDAR data for analysis, LIDAR ground returns must first be separated from vegetation returns. Ground returns were identified by the LIDAR vendor, with the exception of the Clear Creek LIDAR unit ground returns, which were classified with MCC-LiDAR (Evans and Hudak 2007). We rasterized ground returns to

Table 1. Summary of Light Detection and Ranging (LIDAR) acquisitions and plot data used in developing cover board models for Nez Perce–Clearwater National Forest, Idaho, USA, 2009–2015.

LIDAR collection	Area (ha)	LIDAR pulse density (1st returns/m^2)	LIDAR year	No. plots	Plot year
Clear Creek	17,335	4.5	2009	4[a]	2015
Crooked River	19,223	7.7	2012	5[a]	2015
Dutch Oven	3,106	17.7	2014	2[a]	2015
Lolo Creek–El Dorado Creek	21,314	7.7	2012	5[a]	2015
Powell	53,522	6.1	2011	13[a]	2015
Selway River–Elk Creek	64,988	7.7	2012	9[a]	2015
Twin Creek	5,206	4.7	2009	1[a]	2015
French Creek–North Fork	38,788	7.7	2012	161[b]	2014

[a] Plot(s) used in model construction.
[b] Plots used in model validation.

Table 2. Description of candidate predictor variables considered when constructing horizontal-cover models for the Nez Perce–Clearwater National Forest, Idaho, USA, 2009–2015. All Light Detection and Ranging (LIDAR) heights were normalized and refer to height above ground.

Name	Description
H05	5th percentile of LIDAR heights
H25	25th percentile of LIDAR heights
H50	50th percentile of LIDAR heights
H75	75th percentile of LIDAR heights
H95	95th percentile of LIDAR heights
Hmean	Mean LIDAR height
Hsd	Standard deviation of LIDAR heights
Hsk	Skewness of LIDAR heights
CCR	Canopy relief ratio
Stratum 0 Prop	Proportion of LIDAR returns <0.15 m
Stratum 1 Prop	Proportion of LIDAR returns ≥0.15 m and <2.0 m
Stratum 1 Ku	Kurtosis of LIDAR returns ≥0.15 m and <2.0 m
Stratum 1 Sk	Skewness of LIDAR returns ≥0.15 m and <2.0 m
Stratum 2 Prop	Proportion of LIDAR returns ≥2.0 m and <5.0 m
Stratum 3 Prop	Proportion of LIDAR returns ≥5.0 m
LIDAR Age	Years between LIDAR acquisition and field measurements

create 1-m-resolution digital terrain models (DTMs). We height-normalized LIDAR returns by subtracting the DTM from the LIDAR returns' *z*-value resulting in height-above-ground for each LIDAR return. We extracted height-normalized LIDAR returns located within the fixed-area plots and used these to create numerous LIDAR metrics that describe 3-dimensional vegetation structure. The possible number of metrics that could be computed is excessive, so we calculated a set of metrics that were expected to relate to understory vegetation that would obscure the cover board. The selected metrics focused on, but were not limited to, LIDAR returns that were close to the ground and included height metrics, strata metrics, canopy relief ratio (McGaughey 2016), and LIDAR Age (Table 2; Tables S1 and S2, available online in Supporting Information). We calculated height metrics from all LIDAR first returns >0.15 m above-ground—this height cutoff limits the metrics to vegetation returns. We calculated strata metrics from subsets of LIDAR returns located within a user-specified height range above the ground. We choose to calculate metrics for 4 strata: Stratum 0—LIDAR returns close to the ground, Stratum 1—LIDAR returns in the height range of the cover board, and Strata 2 and 3—LIDAR returns directly above the cover board. Canopy relief ratio represented surface texture. The final metric, LIDAR Age, represented the number of years between LIDAR collections and the field data. These 16 LIDAR metrics were used as predictor variables for the candidate models (Table 2). All LIDAR processing was done using FUSION (FUSION Version 3.50, http://forsys.cfr.washington.edu/fusion/fusion_overview.html, accessed 10 Jun 2016).

Horizontal Cover Models

We bound horizontal cover estimates between zero (completely visible) and one (completely obscured), which is an important consideration in selecting a modelling technique. Beta regression is an extension of generalized linear models (GLM) where the error distribution can be described by the beta distribution, a 2-parameter function bound by 0 and 1 that can take on many shapes (Ferrari and Cribari-Neto 2004). A beta distribution is advantageous in our case because the variance of horizontal cover is expected to be nonnormal, especially near the extremes (0 and 1). As with GLM, a link function relates the predictor variables to the response variable; several link functions are available with beta regression, and we selected the logit (Equation 1),

$$\log_e\left(\frac{\mu}{1-\mu}\right) = \eta = \sum x_j\beta_j, \qquad (1)$$

where η is a linear combination of predictor variables (x_j) and regression coefficients (β_j). We obtained horizontal cover predictions (μ) from the inverse of the logit function (Equation 2).

$$\mu = \frac{\exp(\eta)}{1+\exp(\eta)} \qquad (2)$$

We created beta regression models in R statistical software (R Version 3.5.0, www.r-project.org, accessed 19 Jun 2018) using the betareg package (Cribari-Neto and Zeileis 2010, Grün et al. 2012). An important consideration in selecting predictor variables is identifying multicollinear predictor variables; removing these multicollinear variables was therefore necessary to create an ecologically meaningful model. Failure to remove multicollinear predictor variables confounds the interpretation of the model coefficients (Graham 2003). When 2 candidate predictor variables exhibited a Spearman's rank coefficient $>|0.7|$, the variable that directly measured vegetation between 0.15 m and 2.0 m remained and we excluded the other from the list of predictor variables. To ensure that no multicollinear variables remained, we calculated the variance inflation factor (VIF) for the remaining candidate variables, ensuring the VIF was <2. Only 41 observations were available for fitting a model, so we only tested univariate and bivariate candidate models. Interaction terms in the bivariate models were retained when found to be statistically significant ($P < 0.05$). We selected the final models based on the smallest corrected Akaike Information Criteria (AIC_c), which is a bias-corrected extension of the AIC suitable for small sample sizes (Hurvich and Tsai 1989). We also considered interaction terms for bivariate candidate models. We constructed 4 beta regression models, which we named according to the threshold used when selecting photos blocked by tree boles: AT—all photos were used regardless of whether a tree bole was blocking the cover board; LT75—photos were excluded when a tree bole blocked >75% of the cover board; LT50—photos were excluded when a tree bole blocked >50% of the cover board; and LT25—photos were excluded when a tree bole blocked >25% of the cover board. Model AT represented the current cover board scoring procedure used by the USFS in the Northern Region.

We assessed beta regression models with fit statistics including pseudo-R^2 value, which is the square of the correlation between η and the link function (Ferrari and Cribari-Neto 2004), relative mean bias (MB%; Equation 3), and relative root mean square error (RMSE%; Equation 4).

$$\text{MB\%} = \frac{\sum(\text{predictions} - \text{observations})}{\text{mean(observations)}} \times 100\% \quad (3)$$

$$\text{RMSE\%} = \frac{\sqrt{\frac{1}{n}\sum(\text{predictions} - \text{observations})^2}}{\text{mean(observations)}} \times 100\% \quad (4)$$

Likewise, we calculated performance statistics of R^2, MB%, and RMSE% when the final models were applied to the validation data. Plots of predicted versus observed horizontal-cover estimates are also presented.

RESULTS

We constructed 4 horizontal cover models; each model represented the effect of removing cover board photos obscured by tree boles from the training data set. We constructed all final models using 2 predictor variables; interaction terms were not significant in the final models (Table 3). The selected model AT, which did not exclude cover board photos obscured by tree boles, was constructed from Stratum 2 Prop (Proportion of returns ≥2.0 m and <5.0 m) and LIDAR Age. The second-ranked candidate model AT was constructed from Stratum 1 Prop (Proportion of returns ≥0.15 m and <2.0 m) and Stratum 2 Prop. The practical difference between these 2 AIC_c values was null (0.1). The 3 models that excluded photos blocked by tree boles were constructed from Stratum 1 Prop and Stratum 2 Prop. Recall, the cover board was 2.0 m tall and these strata LIDAR metrics relate to the area in the plane of the cover board and directly above (Table 2).

Scatter plots of predicted versus observed horizontal-cover measurements for both the training data and validation data show similar spread around the 1-to-1 line among models (Figs. 3, 4). With the exception of model AT, fit statistics based on training data were similar to the performance statistics calculated from the validation data (Figs. 3, 4). The MB% for the training data were all slightly negative (−0.4 to −0.8%), while the validation model MB% for AT was −18.5% and the remaining 3 models were slightly positive (2.2–3.6%; Fig. 3). The fit statistic RMSE% calculated from the training data ranged between 30.8% and 33.7%, while the performance RMSE% calculated using the validation data was substantially lower at 24.6–33.5% (Fig. 4). Models that excluded photos blocked by tree boles saw improved performance statistics compared with model AT, providing justification to remove photos that were not representative of the plot.

Table 3. Corrected Akaike Information Criterion (AIC_c) for univariate, bivariate, and global beta regression models used to predict understory cover on the Nez Perce–Clearwater National Forest, Idaho, USA, 2009–2015. Global model was constructed from H05, Stratum 0 Prop, Stratum 1 Prop, Stratum 1 Sk, Stratum 2 Prop, and Light Detection and Ranging (LIDAR) Age. Models with the minimum AIC_c values were selected.

		AIC_c			
Predictor variables		**AT**	**LT75**	**LT50**	**LT25**
H05[a]		−7.8	−9.4	−7.7	−6.8
Stratum 0 Prop[b]		1.4	2.5	3.5	4.1
Stratum 1 Prop[c]		−17.8	−21.3	−20.6	−18.7
Stratum 1 Sk[d]		−3.9	−2.9	−2.2	−1.7
Stratum 2 Prop[e]		−28.3	−33.6	−31.3	−29.4
LIDAR Age[f]		−2.1	−0.3	1.0	1.4
H05	Stratum 0 Prop	−5.6	−7.2	−5.5	−4.7
H05	Stratum 1 Prop	−17.1	−21.8	−20.6	−18.7
H05	Stratum 1 Sk	−6.6	−8.0	−6.5	−5.7
H05	Stratum 2 Prop	−26.6	−33.0	−30.4	−28.4
H05	LIDAR Age	−7.4	−8.6	−6.6	−5.7
Stratum 0 Prop	Stratum 1 Prop	−16.9	−20.6	−20.1	−18.5
Stratum 0 Prop	Stratum 1 Sk	−2.1	−1.5	−0.7	0.0
Stratum 0 Prop	Stratum 2 Prop	−26.1	−31.7	−29.2	−27.2
Stratum 0 Prop	LIDAR Age	−0.1	1.4	2.8	3.4
Stratum 1 Prop	Stratum 1 Sk	−21.3	−25.9	−25.6	−23.5
Stratum 1 Prop	Stratum 2 Prop	−31.8	−40.6[g]	−38.7[g]	−35.8[g]
Stratum 1 Prop	LIDAR Age	−18.6	−21.7	−20.5	−18.6
Stratum 1 Sk	Stratum 2 Prop	−26.1	−31.4	−29.2	−27.4
Stratum 1 Sk	LIDAR Age	−3.9	−2.4	−1.4	−0.9
Stratum 2 Prop	LIDAR Age	−31.9[g]	−31.9	−34.0	−32.0
Global		−26.8	−35.9	−33.7	−32.8

[a] H05: 5th percentile of LIDAR heights.
[b] Stratum 0 Prop: Proportion of LIDAR returns <0.15 m.
[c] Stratum 1 Prop: Proportion of LIDAR returns ≥0.15 m and <2.0 m.
[d] Stratum 1 Sk: Skewness of LIDAR returns ≥0.15 m and <2.0 m.
[e] Stratum 2 Prop: Proportion of LIDAR returns ≥2.0 m and <5.0 m.
[f] LIDAR Age: Years between LIDAR acquisition and field measurements.
[g] Selected model.

Beta regression model parameters are interpreted as odds ratio; therefore, the effect of a new measurement on horizontal cover can be explored for a given predictor variable (Table 4). For example, consider the Stratum 1 Prop coefficient for LT75, which was 2.85. Holding all else constant, a 0.10 increase in Stratum 1 Prop results in a 1.329 times increase [$\exp(2.85 \times 0.10) = 1.329$] in the odds ratio (i.e., $\mu^*/(1 - \mu^*)/\mu/(1 - \mu)$, where μ is the original prediction and μ^* is the new prediction).

DISCUSSION

We demonstrated that LIDAR-based models can predict horizontal cover, similar to traditional cover boards, with the benefit of making predictions across spatial extents much larger than are typically surveyed with field measurements. Final models performed well (e.g., RMSE% of 30.8–33.7%) and an independent validation data set confirmed these results (e.g., RMSE% of 24.6–33.5%).

Model Development

We demonstrated that excluding cover board photos where the tree bole was responsible for the obstruction resulted in improved model results. Horizontal cover estimates calculated by averaging cover board estimates from 4 photos

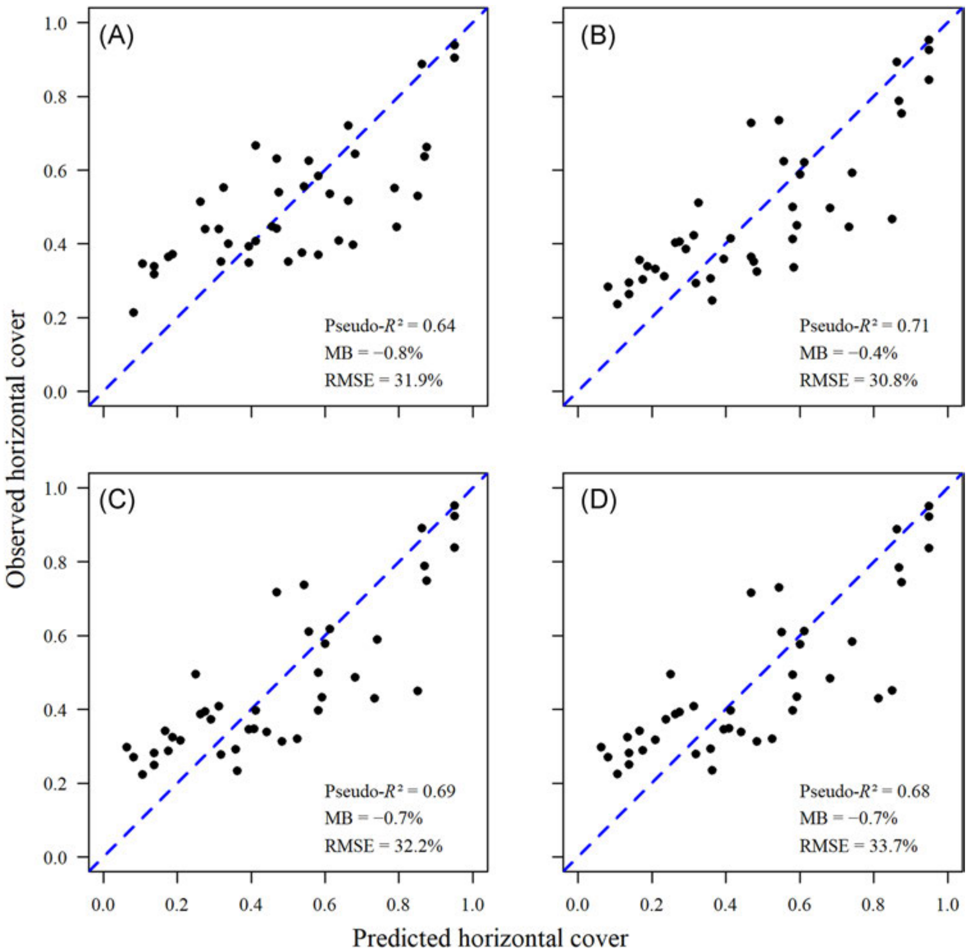

Figure 3. Relationship between predicted and observed horizontal-cover estimates based on training data collected on the Nez Perce–Clearwater National Forest, Idaho, USA, 2009–2015. (A) Model AT, (B) model LT75, (C) model LT50, and (D) model LT25. Model fit statistics included pseudo-R^2, mean bias (MB), and root mean square error (RMSE).

partially ameliorates these unrepresentative measurements. Campbell et al. (2018) also noted that a single tree bole could obscure a cover board; however, in that study 25 photos of a single cover board were taken along a grid, whereas in this study only one photograph was taken per cover board. We found that excluding photos where a tree bole obscured ≥75% of the cover board improved the model fit and performance statistics. This modification to the cover board scoring procedure can be done in the laboratory and is not expected to increase the time to score the photo. An in-field alternative could be to shift the cover board location by 45° (e.g., from north to northeast), but this would require the field crew to visit more locations in the field, potentially bias the measurements, and not guarantee a new location would not be blocked by a new tree bole.

Model Application

We created a statistical model by combining geolocated field data and plot-level LIDAR data. Light Detection and Ranging data are collected across large spatial extents and can be processed to generate maps of gridded metrics across the entire LIDAR extent. These maps are typically created at 20-m or 30-m resolution. The LIDAR-based prediction models can be applied to gridded LIDAR metrics resulting in horizontal cover maps spanning the entire LIDAR collection (Fig. 5).

Predictive modeling of horizontal cover using LIDAR measurements could provide an assessment of horizontal cover without the need to field-evaluate all multistoried stands within mapped Canada lynx habitat. Analysis of horizontal cover using LIDAR could provide better informed sample locations, thus expanding the area of land being more efficiently sampled by focusing limited resources. It would also allow assessment of horizontal cover at a much larger spatial scale. Maps depicting LIDAR-modeled horizontal-cover estimates could decrease the time and increase the accuracy in evaluating winter snowshoe hare foraging habitat for project-level analyses, which are required to determine the effects of various vegetation management activities on Canada lynx habitat. Additionally, maps of horizontal cover across an entire project area could aid adaptive project planning, allowing patches of varying habitat quality to be identified and assigned appropriate prescriptions.

Horizontal cover is just one component determining Canada lynx habitat, yet remote-sensing products can be used to

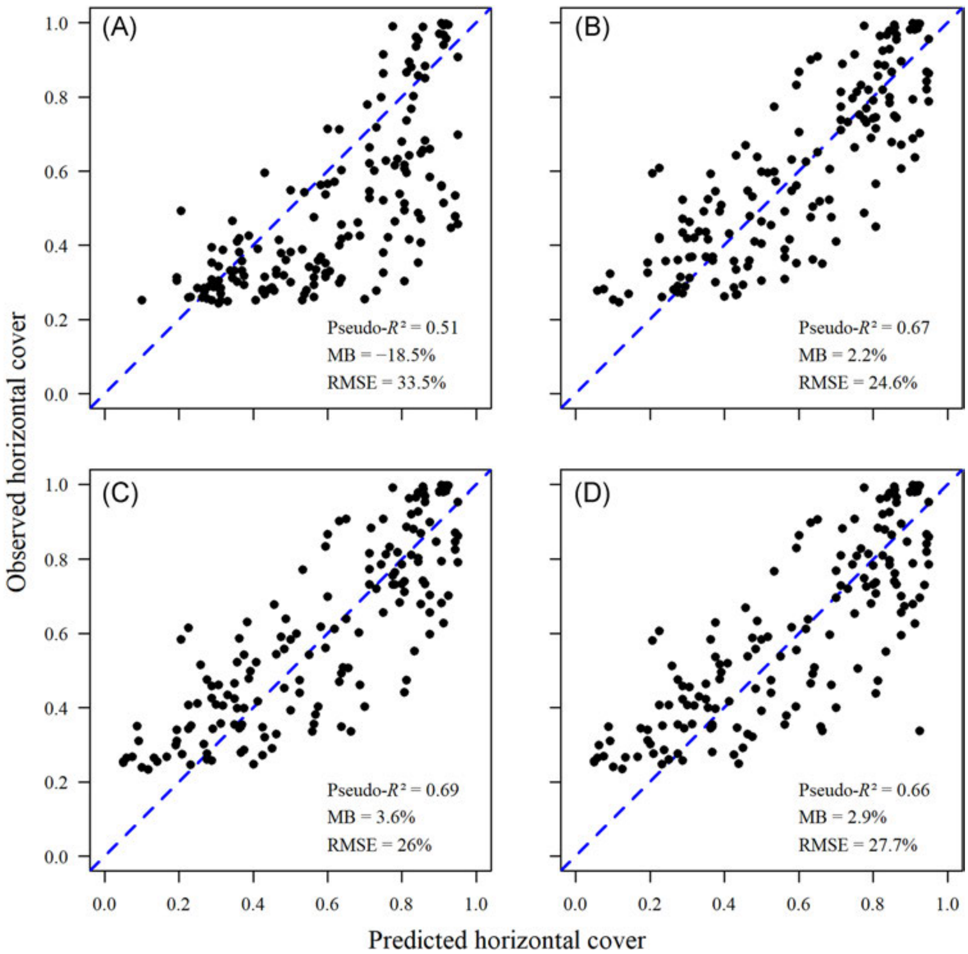

Figure 4. Relationship between predicted and observed horizontal-cover estimates based on validation data, Nez Perce–Clearwater National Forest, Idaho, USA, 2009–2015. (A) Model AT, (B) model LT75, (C) model LT50, and (D) model LT25. Model performance statistics included pseudo-R^2, mean bias (MB), and root mean square error (RMSE).

identify other habitat features. Other components of Canada lynx habitat include forest structural stage, vegetation species present, and snow depth. Light Detection and Ranging metrics and field data have been used to create structural stage models with class accuracies of 87–94% and Cohen's Kappa values of 0.85–0.93 (Falkowski et al. 2009). Holbrook et al. (2017) found a species-specific association between snowshoe hares and abundance of lodgepole pine (*Pinus contorta*). Other components of habitat selected by Canada lynx in the winter include mature, multilayered forests with Engelmann spruce and subalpine fir (*Abies lasiocarpa*) in the midstory and overstory (Holbrook et al. 2017). Tree species identification from

Table 4. Beta regression model parameters used to predict horizontal cover on the Nez Perce–Clearwater National Forest, Idaho, USA, 2009–2015. LIDAR is Light Detection and Ranging.

Model	Regression coeff.	Parameter	Estimate	SE	z-value	Pr(>|z|)
AT	β_0	Intercept	−1.63	0.40	−4.12	0.000
	β_1	Stratum 2 Prop[a]	11.28	1.85	6.08	0.000
	β_2	LIDAR Age[b]	0.25	0.10	2.57	0.010
LT75	β_0	Intercept	−1.17	0.17	−7.01	0.000
	β_1	Stratum 1 Prop[c]	2.85	0.88	3.23	0.001
	β_2	Stratum 2 Prop	10.20	1.98	5.16	0.000
LT50	β_0	Intercept	−1.24	0.17	−7.14	0.000
	β_1	Stratum 1 Prop	3.04	0.92	3.31	0.001
	β_2	Stratum 2 Prop	10.16	2.03	5.00	0.000
LT25	β_0	Intercept	−1.24	0.18	−6.85	0.000
	β_1	Stratum 1 Prop	2.96	0.95	3.11	0.002
	β_2	Stratum 2 Prop	10.17	2.09	4.86	0.000

[a] Stratum 2 Prop: Proportion of LIDAR returns ≥2.0 m and <5.0 m.
[b] LIDAR Age: Years between LIDAR acquisition and field measurements.
[c] Stratum 1 Prop: Proportion of LIDAR returns ≥0.15 m and <2.0 m.

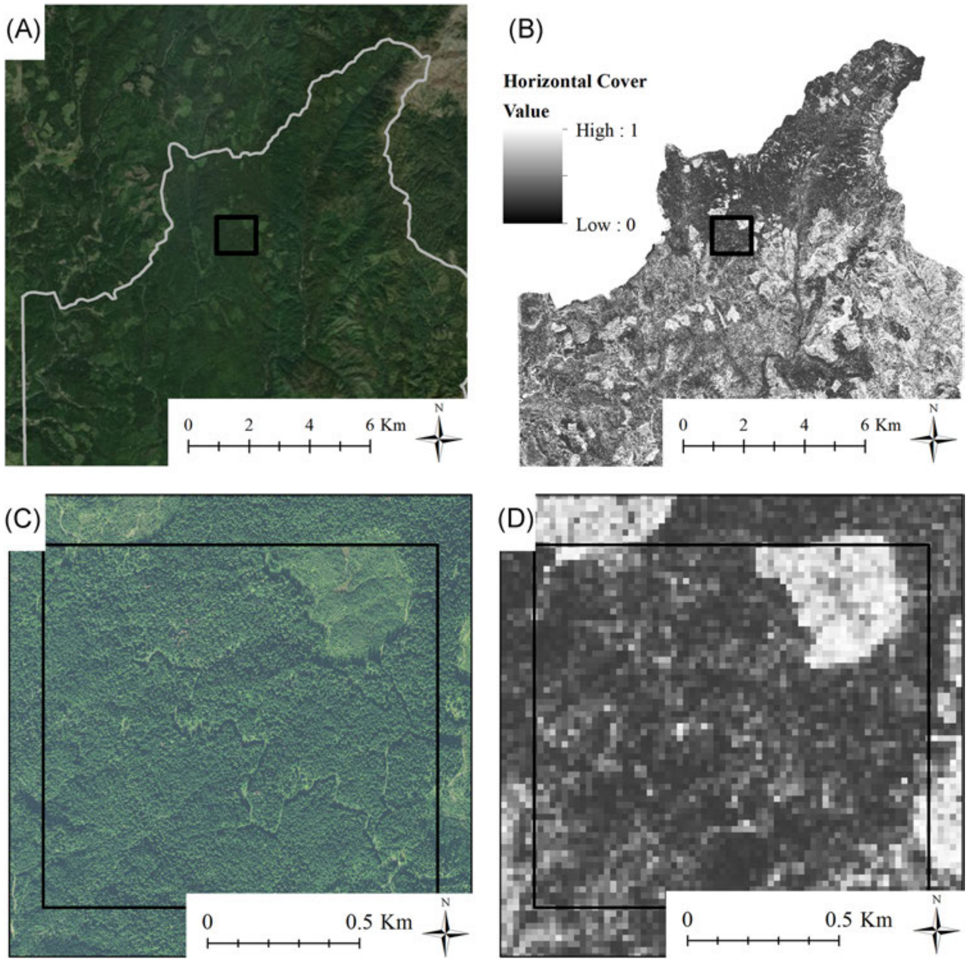

Figure 5. Example of predicted horizontal-cover maps created by applying model LT75 to the Lolo Creek–El Dorado Light Detection and Ranging unit collected in 2012 on the Nez Perce–Clearwater National Forest, Idaho, USA. Corresponding aerial images are included for reference. (A) Aerial image and (B) predicted horizontal cover showing landscape-level patterns. (C) aerial image, and (D) predicted horizontal cover showing stand-level patterns.

LIDAR data alone are often difficult and improved by the addition of aerial imagery (e.g., Holmgren et al. 2008) or satellite imagery (e.g., Nordkvist et al. 2012). Holbrook et al. (2017) used field data, remotely sensed topographic, and Landsat imagery to construct predictive models and map snowshoe hare occupancy and intensity of use across northwest Montana, USA. Incorporating LIDAR-based horizontal-cover metrics into a similar modeling framework may further improve the quality of such comprehensive models, ultimately building a more complete picture of Canada lynx habitat.

Forest Dynamics

It should be noted that horizontal cover is not static, but changes on intra- and interannual time scales. Indeed, it has been recommended that summer and winter measurements have different acceptable horizontal-cover limits for Canada lynx habitat (Bertram and Claar 2009). Consequently, the timing of data collection must be considered. Our field plots were measured in summer, reducing intraseasonal mismatch between LIDAR data and cover board measurements. Light Detection and Ranging data are collected over a short period of time, usually a few days; therefore, those LIDAR data only represent the vegetation during that time period. On an intra-annual scale, deciduous shrubs alter between a leaf-on and leaf-off state, which can greatly affect horizontal cover. Light Detection and Ranging on the NPCNF was collected in snow-off periods, when deciduous shrubs have leaves and understory shrubs will reflect a larger proportion of LIDAR returns. Combining LIDAR collected in leaf-on and leaf-off states is not advised when modeling understory horizontal cover because many understory shrubs in these coniferous forests are deciduous. Likewise, winter and summer cover board measurements should not be mixed.

Habitat selected by Canada lynx also changes between winter and summer. In winter, Squires et al. (2010) found Canada lynx are more likely to be found in multistory forests where conifer branches contributed the most to high horizontal-cover density. In summer, Canada lynx select forests with high horizontal cover characterized by abundant shrubs, small diameter trees, and dense saplings (Squires et al. 2010). The current cover board scoring procedure used by the USFS in the Northern Region does not record the object that is providing the cover, but doing so could help distinguish between selected winter and summer Canada lynx habitat in addition to identifying photos blocked by tree boles.

On longer timescales, horizontal cover will change as a result of forest succession. The trajectory of a forest stand depends on the initial stand conditions along with natural events and management activities. In the Rocky Mountains, wildland fire is a predominant natural driver of forest development, while humans influence stand development through silvicultural activities such as thinnings and harvests (Arno 1980, Cooper et al. 1991). The USFS restricts certain silvicultural activities, such as precommercial thinning in the stand initiation structural stage, if doing so reduces winter snowshoe hare habitat (USDA Forest Service 2007). These decisions effectively maintain horizontal cover and increase the duration that a stand will be potential snowshoe hare habitat. Under certain scenarios, snowshoe hare densities can increase after prescribed burning in lodgepole pine stands (Cheng et al. 2010). Young, dense lodgepole pine offer high horizontal cover for snowshoe hares, although these forests make poor denning habitat for Canada lynx (Squires et al. 2008).

Light Detection and Ranging Cost Considerations

A major constraint of implementing a LIDAR-based estimate of horizontal cover is acquiring the LIDAR data. We were fortunate to have access to existing LIDAR data sets to test our study objectives. The cost to acquire new LIDAR data is affected by numerous factors including mobilization cost, topography, area flown, and collection parameters such as pulse density. Every LIDAR acquisition is unique; therefore, few published data on the cost of LIDAR data exist. Hummel et al. (2011) compared the cost of acquiring forest inventory data (e.g., basal area) using a LIDAR-modeling approach and traditional field-based approach and found the 2 strategies comparable in cost and accuracy. Hummel et al. (2011) reported that 2007 LIDAR cost US$42,700 for 12,800 ha (US$3.34/ha); however, LIDAR technology has improved and cost has decreased. Recent cost estimates for LIDAR located in the vicinity of our study area ranged from US$1.25/ha to US$2.75/ha depending on project-specific factors.

Light Detection and Ranging is used to meet multiple objects, like creating a high-quality DTM for flood plain mapping; therefore, cost-sharing opportunities arise within or among external agencies, such as Federal Emergency Management Agency or U.S. Geological Survey. Additionally, scenarios may arise where resource managers have the opportunity to partially fund a planned LIDAR collection to increase the LIDAR quality level (e.g., increasing the pulse density).

MANAGEMENT IMPLICATIONS

In the Rocky Mountains, identifying Canada lynx habitat is a complex process, required by law, and a horizontal cover model can be an important component. This research demonstrates the ability of LIDAR-based models to predict horizontal cover estimates useful for wildlife management. Light Detection and Ranging is collected across large spatial extents, so maps of horizontal estimates can be produced, which can assist in Canada lynx management along with other species. Maps could be used to identify areas of quality habitat or assist in determining field sampling intensity, reducing time and effort in the field. Light Detection and Ranging–derived horizontal-cover maps are not meant to totally replace field sampling, but can provide managers information to better identify potential snowshoe hare habitat at a greater spatial scale and provide guidance when selecting field sampling locations. Doing so may allow managers to sample larger areas by identifying forest stands that do not need to be sampled. In addition, analysis of horizontal cover using LIDAR has applicability beyond Canada lynx conservation because snowshoe hares are prey for other predators in the forests of North America (Krebs et al. 1995).

ACKNOWLEDGMENTS

We thank C. Hickey for providing the validation data and C. DeLay and D. Roberts for assistance in collecting the training data. We thank J. C. Vogeler for productive discussions in habitat modeling. Finally, we thank the Associate Editor and an anonymous reviewer for providing comments that improved the manuscript. This work was funded by the U.S. Forest Service Nez Perce–Clearwater National Forest through an In Service Agreement (ISA 0117-15-010) to the Idaho Department of Fish and Game (contract # AG-03R6-C-14-0056) and the NASA Carbon Monitoring Systems Program (Award NNH15AZ06I) through a Joint Venture Agreement (16-JV-11221633-061).

LITERATURE CITED

American Society for Photogrammetry & Remote Sensing [ASPRS]. 2013. LAS specification version 1.4-R13. <http://www.asprs.org/a/society/committees/standards/LAS_1_4_r13.pdf>. Accessed 12 Nov 2018.

Arno, S. F. 1980. Forest fire history in the Northern Rockies. Journal of Forestry 78:460–465.

Berg, N. D., E. M. Gese, J. R. Squires, and L. M. Aubry. 2012. Influence of forest structure on the abundance of snowshoe hares in western Wyoming. Journal of Wildlife Management 76:1480–1488.

Bertram, T., and J. Claar. 2009. Horizontal cover—interim guidance for assessing multi-storied stands within lynx habitat, revised version, 12 August 2009. U.S. Forest Service unpublished report, Missoula, Montana, USA.

Campbell, M. J., P. E. Dennison, A. T. Hudak, L. M. Parham, and B. W. Butler. 2018. Quantifying understory vegetation density using small-footprint airborne lidar. Remote Sensing of Environment 215:330–342.

Cheng, E., H. K. E. Hodges, and L. S. Mills. 2010. Impacts of fire on snowshoe hares in Glacier National Park, Montana, USA. Fire Ecology 6:13–35.

Cooper, S. V., K. E. Neiman, and D. W. Roberts. 1991. Forest habitat types of northern Idaho: a second approximation. U.S. Department of Agriculture, Forest Service, GTR INT-236, Odgen, Utah, USA.

Cribari-Neto, F., and A. Zeileis. 2010. Beta regression in R. Journal of Statistical Software 34(2):1–24.

Dubayah, R. O., and J. B. D. Drake. 2000. Lidar remote sensing for forestry. Journal of Forestry 6:44–46.

Elton, C., and M. Nicholson. 1942. The ten-year cycle in numbers of the lynx in Canada. British Ecological Society 11:215–244.

Evans, J. S., and A. T. Hudak. 2007. A multiscale curvature algorithm for classifying discrete return LiDAR in forested environments. IEEE Transactions on Geoscience and Remote Sensing 45:1029–1038.

Falkowski, M. J., J. S. Evan, S. Martinuzzi, P. E. Gessler, and A. T. Hudak. 2009. Characterizing forest succession with lidar data: an evaluation for the Inland Northwest, USA. Remote Sensing of Environment 113:946–956.

Ferrari, S. L. P., and F. Cribari-Neto. 2004. Beta regression for modelling rates and proportions. Journal of Applied Statistics 31:799–815.

Goetz, S., D. Steinberg, R. Dubayah, and B. Blair. 2007. Laser remote sensing of canopy habitat heterogeneity as a predictor of bird species richness in an eastern temperate forest, USA. Remote Sensing of Environment 108:254–263.

Graham, M. H. 2003. Confronting multicollinearity in ecological multiple regression. Ecology 84:2809–2815.
Grün, B., I. Kosmidis, and A. Zeileis. 2012. Extended beta regression in R: shaken, stirred, mixed, and partitioned. Journal of Statistical Software 48(11):1–25.
Hagar, J. C. 2007. Wildlife species associated with non-coniferous vegetation in Pacific Northwest conifer forests: a review. Forest Ecology and Management 246:108–122.
Hodges, K. E., L. S. Mills, and K. M. Murphy. 2009. Distribution and abundance of snowshoe hares in Yellowstone National Park. Journal of Mammalogy 90:870–878.
Hodson, J., D. Fortin, L. Bélanger, and É. Renaud-Roy. 2012. Browse history as an indicator of snowshoe hare response to silvicultural practices adapted for old-growth boreal forests. Écoscience 19:266–284.
Holbrook, J. D., J. R. Squires, L. E. Olson, R. L. Lawrence, and S. L. Savage. 2017. Multiscale habitat relationships of snowshoe hares (*Lepus americanus*) in the mixed conifer landscape of the Northern Rockies, USA: cross-scale effects of horizontal cover with implications for forest management. Ecology and Evolution 7:125–144.
Holmgren, J., Å. Persson, and U. Söderman. 2008. Species identification of individual trees by combining high resolution LiDAR data with multi-spectral images. International Journal of Remote Sensing 29:1537–1552.
Hummel, S., A. T. Hudak, E. H. Uebler, M. J. Falkowski, and K. A. Megown. 2011. A comparison of accuracy and cost of LiDAR versus stand exam data for landscape management on the Malheur National Forest. Journal of Forestry 109:267–273.
Hurvich, C. M., and C. L. Tsai. 1989. Regression and time series model selection in small samples. Biometrika 76:297–307.
Ivan, J. S., G. C. White, and T. M. Shenk. 2014. Density and demography of snowshoe hares in central Colorado. Journal of Wildlife Management 78:580–594.
Jones, R. E. 1968. A board to measure cover used by prairie grouse. Journal of Wildlife Management 32:28–31.
Kramer, H., B. Collins, F. Lake, M. Jakubowski, S. Stephens, and M. Kelly. 2016. Estimating ladder fuels: a new approach combining field photography with LiDAR. Remote Sensing 8(9):766.
Krebs, C. J., S. Boutin, R. Boonstra, A. R. E. Sinclair, J. N. M. Smith, M. R. T. Dale, K. Martin, and R. Turkington. 1995. Impact of food and predation on the snowshoe hare cycle. Science 269:1112–1115.
Lewis, C. W., K. E. Hodges, G. M. Koehler, and L. S. Mills. 2011. Influence of stand and landscape features on snowshoe hare abundance in fragmented forests. Journal of Mammalogy 92:561–567.
Martinuzzi, S., L. A. Vierling, W. A. Gould, M. J. Falkowski, J. S. Evans, A. T. Hudak, and K. T. Vierling. 2009. Mapping snags and understory shrubs for a LiDAR-based assessment of wildlife habitat suitability. Remote Sensing of Environment 113:2533–2546.
McGaughey, R. J. 2016. FUSION/LDV: software for LIDAR data analysis and visualization v.3.60. U.S. Forest Service, Seattle, Washington, USA.
Moreno, S., M. Delibes, and R. Villafuerte. 1996. Cover is safe during the day but dangerous at night: the use of vegetation by European wild rabbits. Canadian Journal of Zoology 74:1656–1660.
Mysterud, A., and E. Ostbye. 1999. Cover as a habitat element for temperate ungulates: effects on habitat selection and demography. Wildlife Society Bulletin 27:385–394.
Næsset, E. 2002. Predicting forest stand characteristics with airborne scanning laser using a practical two-stage procedure and field data. Remote Sensing of Environment 80:88–99.
National Oceanic and Atmospheric Administration [NOAA]. 2019. National Centers for Environmental Information. Normals Monthly Station Details. <https://www.ncdc.noaa.gov/cdo-web/datasets/NORMAL_MLY/stations/GHCND:USC00102875/detail>. Accessed 05 Jun 2019.
Nordkvist, K., A.-H. Granholm, J. Holmgren, H. Olsson, and M. Nilsson. 2012. Combining optical satellite data and airborne laser scanner data for vegetation classification. Remote Sensing Letters 3:393–401.
Nudds, T. D. 1977. Quantifying the vegetative structure of wildlife cover. Wildlife Society Bulletin 5:113–117.
Roberts, D. W., and S. V. Cooper. 1989. Concepts and techniques of vegetation mapping Pages 90–96 *in* D. E. Ferguson, P. Morgan, and F. D. Johnson, editors. Proceedings, land classifications based on vegetation: applications for resource management. General Technical Report INT-257, SAF Publication, 88-06. U.S. Department of Agricultural, Forest Service, Ogden, Utah, USA.
Ruggiero, L. F., K. B. Aubry, S. W. Buskirk, G. Koehler, C. J. Krebs, K. S. McKelvey, and J. R. Squires. 1999. Ecology and conservation of lynx in the United States. U.S. Department of Agriculture, Forest Service, General Technical Report: RMRS-GTR-30WWW, Fort Collins, Colorado, USA.
Schmugge, T. J., W. P. Kustas, J. C. Ritchie, T. J. Jackson, and A. Rango. 2002. Remote sensing in hydrology practicum. Advances in Water Resources 25:1367–1385.
Smith, F. W., and J. N. Long. 1987. Elk hiding and thermal cover guidelines in the context of lodgepole pine stand density. Western Journal of Applied Forestry 2:6–10.
Squires, J. R., N. J. DeCesare, J. A. Kolbe, and L. F. Ruggiero. 2008. Hierarchical den selection of Canada lynx in western Montana. Journal of Wildlife Management 72:1497–1506.
Squires, J. R., N. J. DeCesare, J. A. Kolbe, and L. F. Ruggiero. 2010. Seasonal resource selection of Canada lynx in managed forests of the northern Rocky Mountains. Journal of Wildlife Management 74:1648–1660.
U.S. Department of Agriculture, Forest Service. 2007. Northern Rockies lynx management direction record of decision. U.S. Department of Agriculture, Forest Service, Washington, D.C., USA.
U.S. Department of Agriculture, Forest Service. 2018. Region 1 common stand exam and inventory and monitoring field guide: report 18-8 v6.2. <https://www.fs.fed.us/nrm/documents/fsveg/cse_user_guides/R1_CSE_FG_v2016.pdf>. Accessed 12 Nov 2018.
U.S. Endangered Species Act of 1973, as amended, Pub. L. No. 93-205, 87 Stat. 884 (Dec. 28, 1973). Available: http://www.fws.gov/endangered/esa-library/pdf/ESAall.pdf
U.S. Fish and Wildlife Service. 2000. Department of the Interior status for the contiguous U.S. distinct population segment of the Canada lynx and related rule. Federal Register Volume 65, Washington, D.C., USA. <https://www.federalregister.gov/documents/2000/03/24/00-7145/endangered-and-threatened-wildlife-and-plants-determination-of-threatened-status-for-the-contiguous>. Accessed 12 Nov 2018.
U.S. Fish and Wildlife Service. 2014. Endangered and threatened wildlife and plants; revised designation of critical habitat for the contiguous United States distinct population segment of the Canada lynx and revised distinct population segment boundary. Federal Register Volume 79, Washington, D.C., USA. <https://www.federalregister.gov/documents/2014/09/12/2014-21013/endangered-and-threatened-wildlife-and-plants-revised-designation-of-critical-habitat-for-the>. Accessed 12 Nov 2018.

Associate Editor: Anderson.

SUPPORTING INFORMATION

Additional supporting material may be found in the online version of this article at the publisher's web-site. Files contain the field measurements used to create the horizontal cover models (Table S1) and validate the models (Table S2). The files are in CSV format, which allows for easy reading by common statistical software. Descriptions of the predictor variables can be found in Table 2 of the manuscript, and reprinted in the supplemental docx file.

Additional File 1: Additional Figures and Table

Table S1 – Median current and future MAT and MAP values for the national forests in this study.

Figure S1 – Map of mean annual temperature (MAT) and predicted changes in MAT across the Pacific Northwest USA.

Figure S2 – Map of mean annual Precipitation (MAP) and predicted changes in MAP across the Pacific Northwest USA.

Figure 3S – Simulated results of basal area proportions for select tree species on the Ochoco National Forest.

Figure 4S – Simulated results of basal area proportions for select tree species on the Gifford Pinchot National Forest.

Figure 5S – Simulated results of basal area proportions for select tree species on the Siuslaw National Forest.

Figure S6 – Current and future estimates of plot-level basal area distribution simulated using different levels of the dClim rule on the Ochoco National Forest.

Figure S7 – Current and future estimates of plot-level basal area distribution simulated using different levels of the dClim rule on the Gifford Pinchot National Forest.

Figure S8 – Current and future estimates of plot-level basal area distribution simulated using different levels of the dClim rule on the Siuslaw National Forest.

Table S1. Climate normals for year 1990 and projected climate mean annual temperature and mean annual precipitation for years 2030, 2060, and 2090. Data summaries calculated as the median of 1 arc minute rasters returned by the Climate-FVS server [1] using the Ensemble 6.0 climate scenario.

	MAT (°C)				MAP (mm)			
	Year				Year			
National Forest	1990	2030	2060	2090	1990	2030	2060	2090
Payette NF	2.6	4.1	5.2	6.6	757	766	765	806
Ochoco NF	5.9	7.2	8.3	9.6	406	406	369	417
Gifford Pinchot NF	5.7	7.0	8.1	9.3	2146	2163	2164	2267
Siuslaw NF	10.4	11.4	12.3	13.3	2222	2192	2187	2288

Note: MAT – mean annual temperature
MAP – Mean annual total precipitation

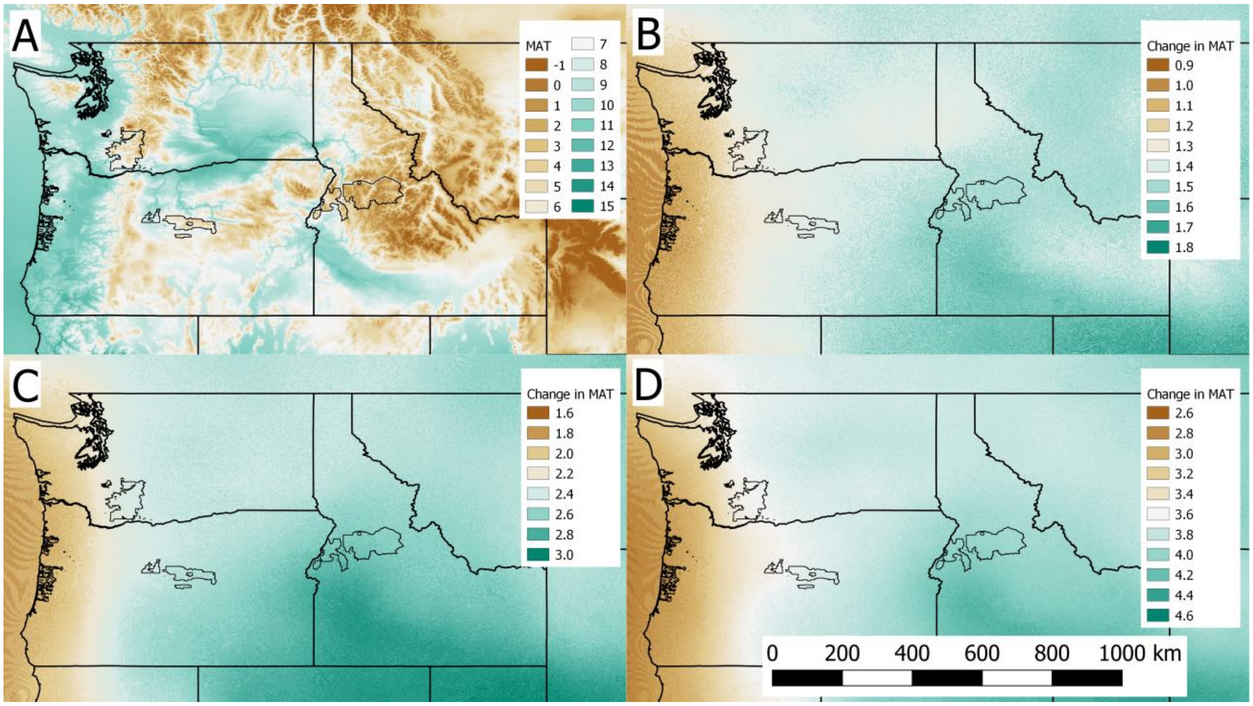

Figure S1. Mean annual temperature (MAT) in °C for (A) northwestern USA in year 1990, and (B) estimated change in MAT used by Climate-FVS under the Ensemble 6.0 climate scenario for years between 1990 and 2030, (C) between 1990 and 2060, and (D) between 1990 and 2090 used by the future climate scenario Ensemble 6.0. Data downloaded from the Climate-FVS server [1].

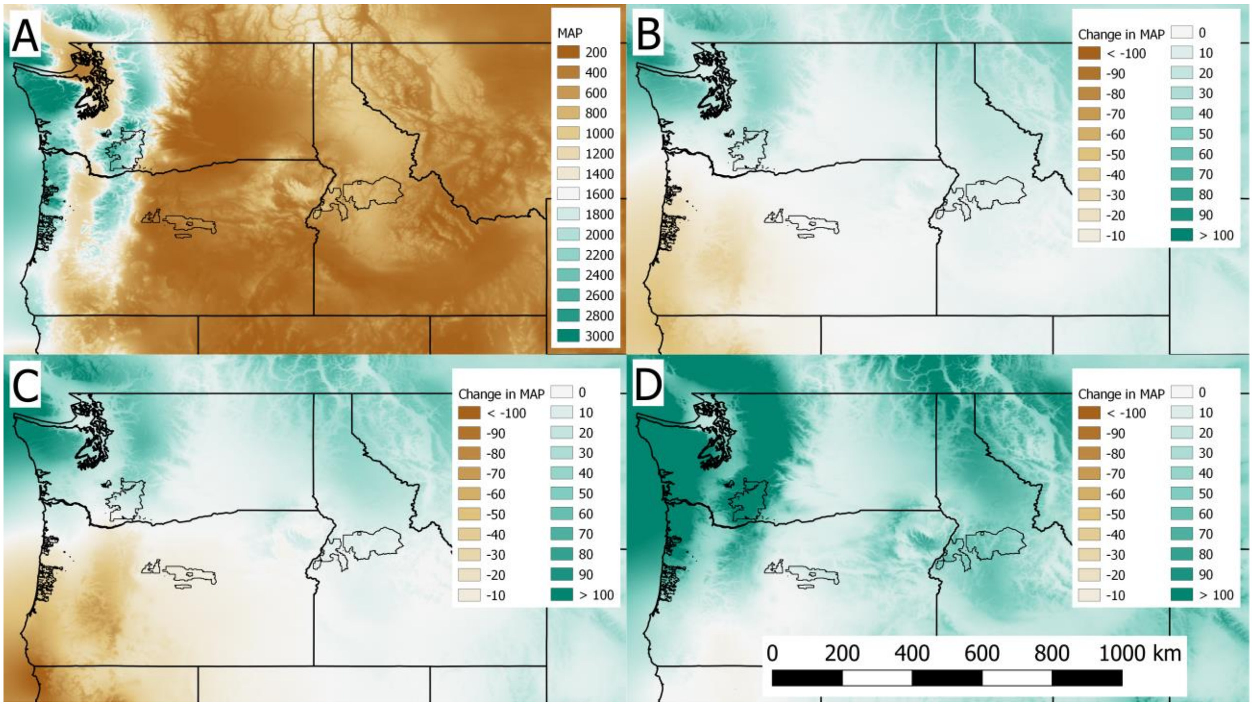

Figure S2. Mean annual precipitation (MAP) in mm for (A) northwestern USA in year 1990, and (B) estimated change in MAP used by Climate-FVS under the Ensemble 6.0 climate scenario for years between 1990 and 2030, (C) between 1990 and 2060, and (D) between 1990 and 2090 used by the future climate scenario Ensemble 6.0. Data downloaded from the Climate-FVS server [1].

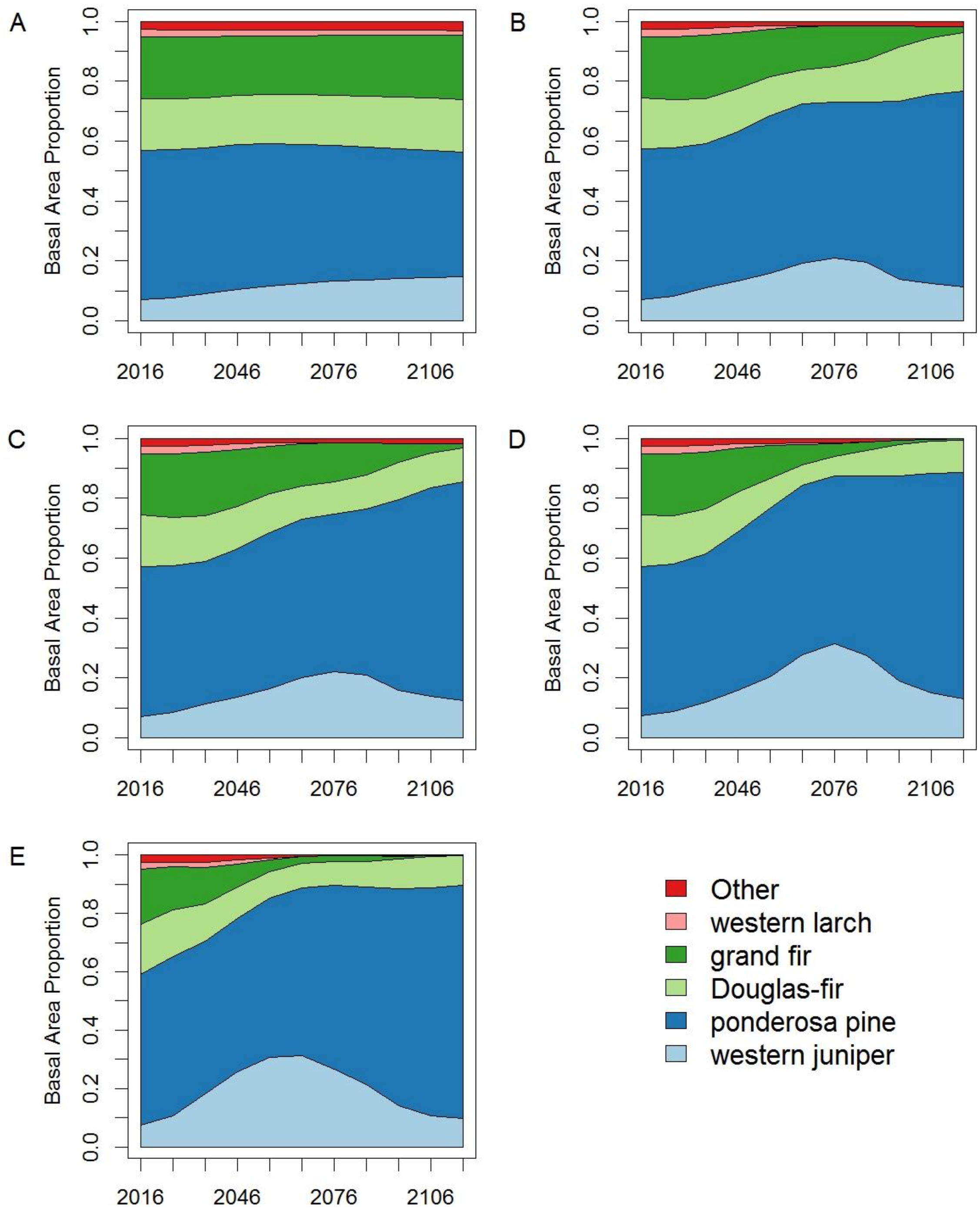

Figure S3: Basal area proportions for select tree species on the Ochoco National Forest simulated with the base disturbance level and: (A) no climate change, (B) dClim Off, (C) dClim 2.0, (D) dClim 1.0 (default setting), and (E) dClim 0.5.

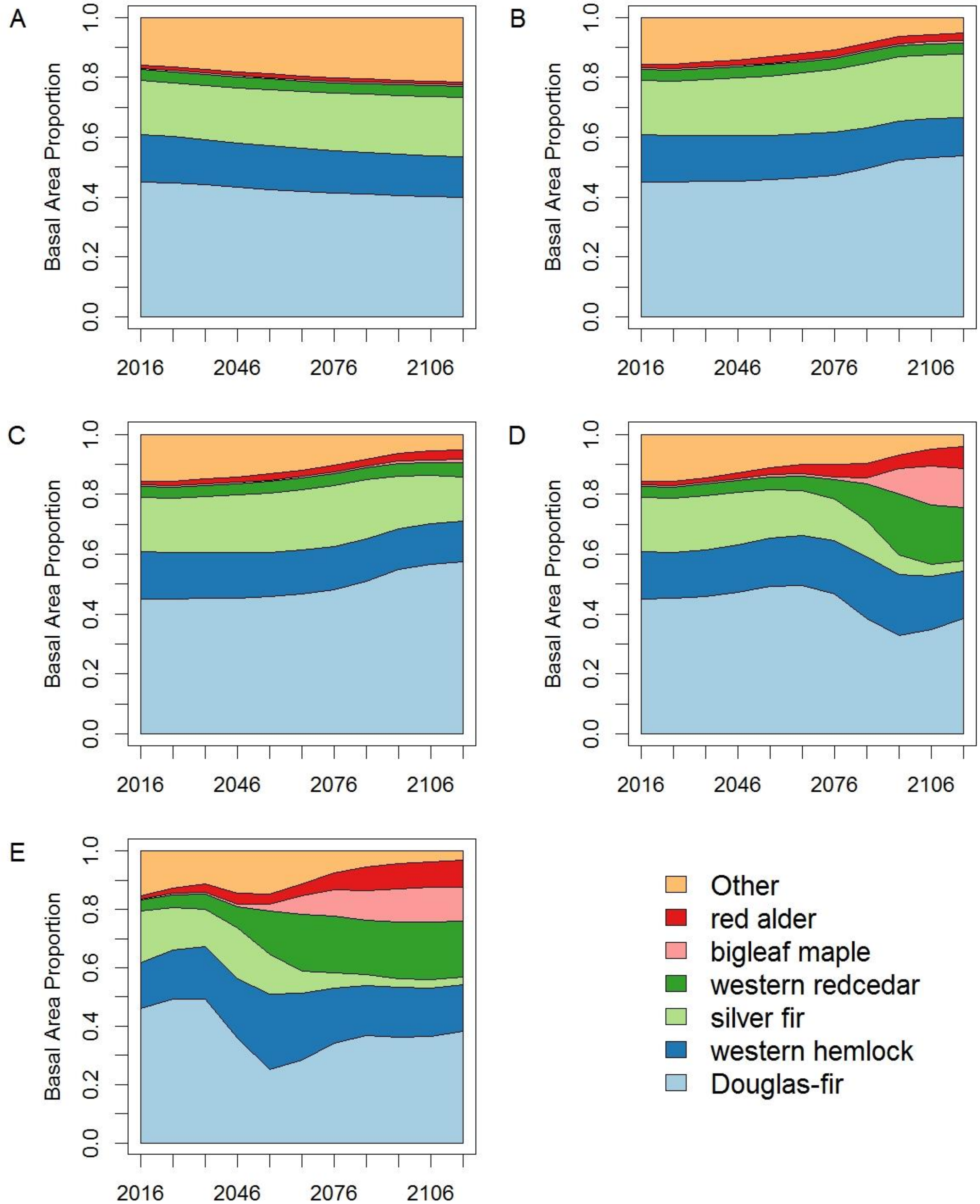

Figure S4: Basal area proportions for select tree species on the Gifford Pinchot National Forest simulated with the base disturbance level and: (A) no climate change, (B) dClim Off, (C) dClim 2.0, (D) dClim 1.0 (default setting), and (E) dClim 0.5.

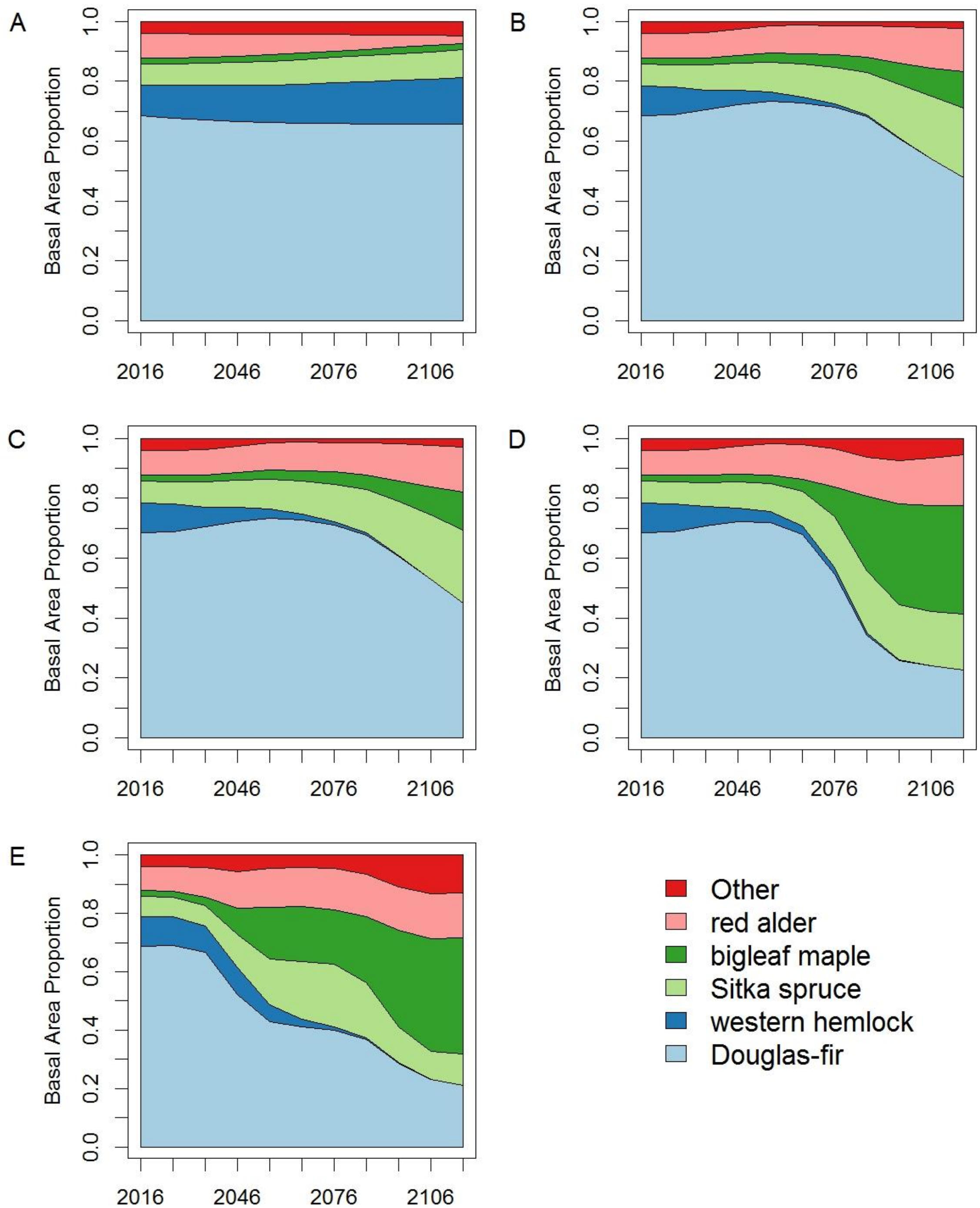

Figure S5: Basal area proportions for select tree species on the Siuslaw National Forest simulated with the base disturbance level and: (A) no climate change, (B) dClim Off, (E) dClim 2.0, (D) dClim 1.0 (default setting), and (E) dClim 0.5.

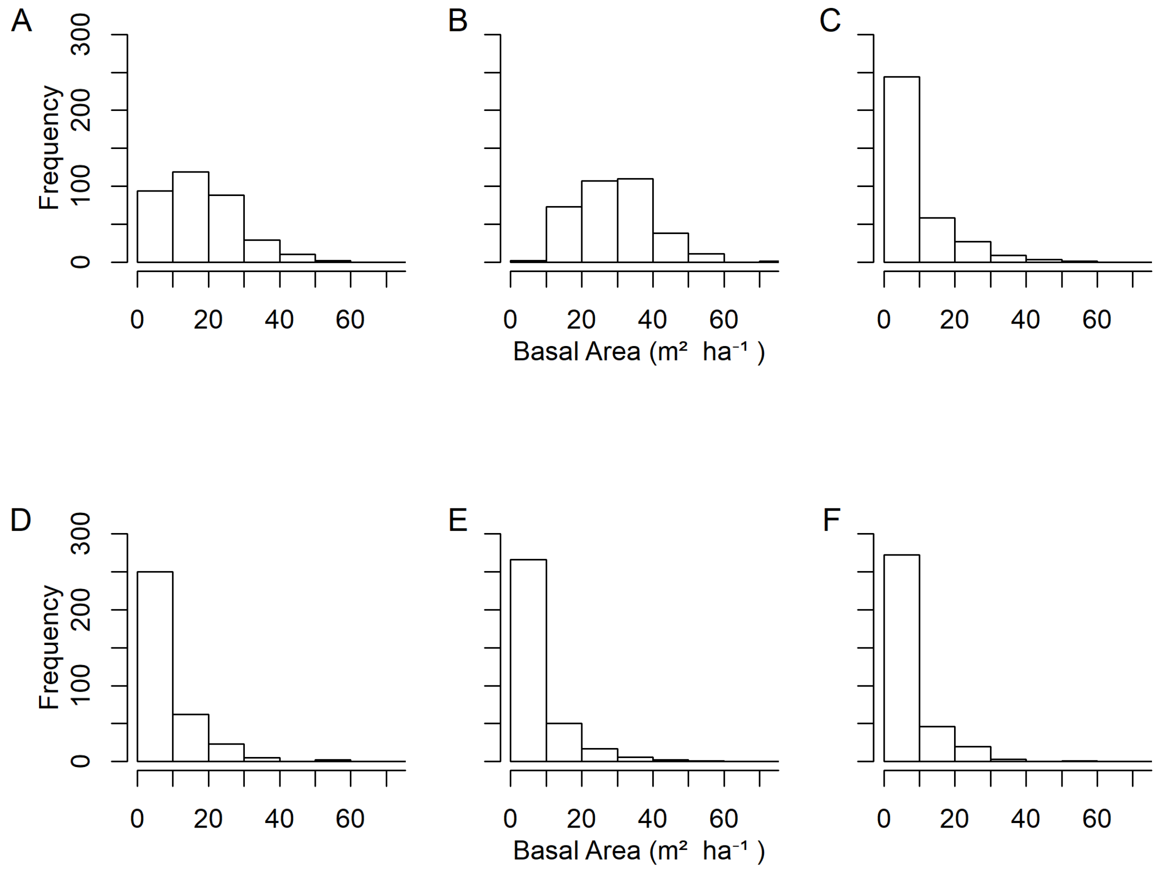

Figure S6: Ochoco National Forest plot-level basal area distribution simulated using the base disturbance level for (A) current conditions (year=2016); (B) future conditions under no climate change (year=2116); (C) future conditions under dClim 2.0 (year=2116); (D) future conditions under dClim Off (year=2116); (E) future conditions under dClim 1.0 (year=2116); (F) future conditions under dClim 0.5 (year=2116).

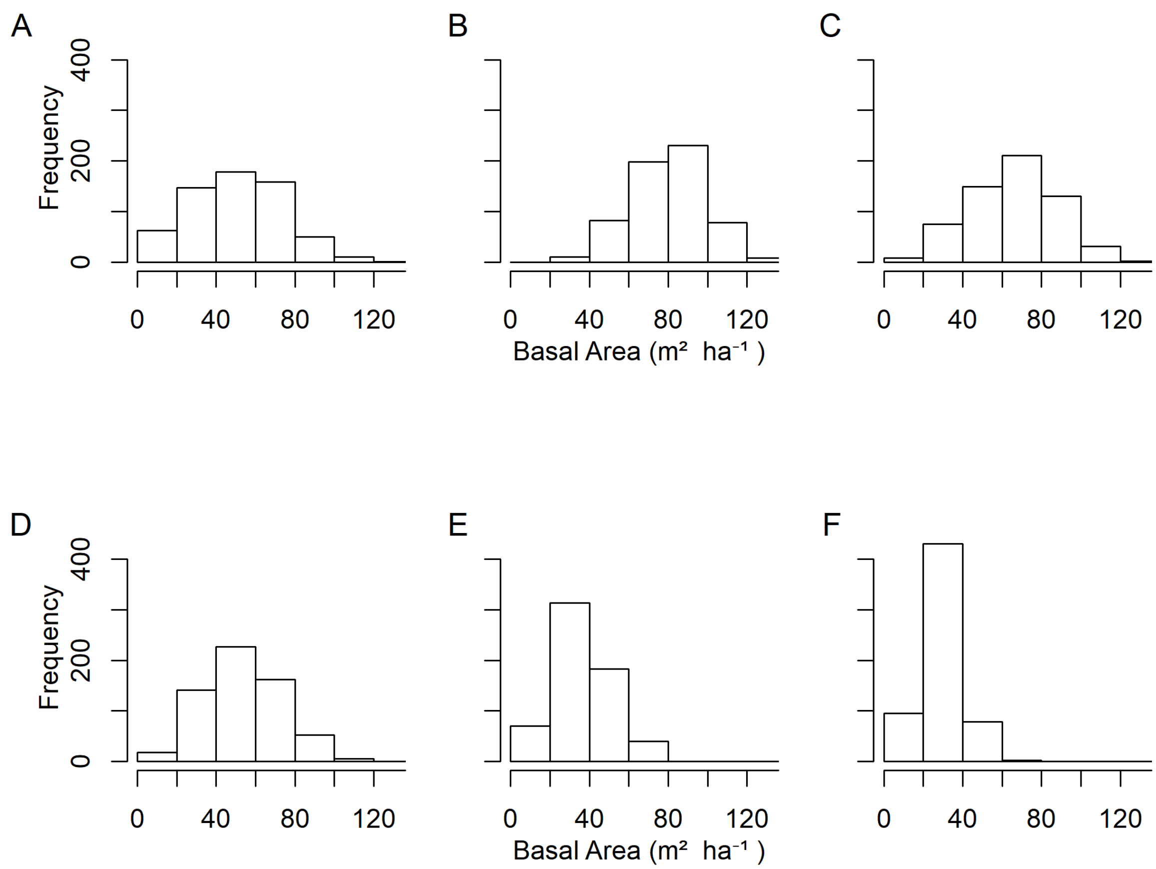

Figure S7: Gifford Pinchot National Forest plot-level basal area distribution simulated using the base disturbance level for (A) current conditions (year=2016); (B) future conditions under no climate change (year=2116); (C) future conditions under dClim 2.0 (year=2116); (D) future conditions under dClim Off (year=2116); (E) future conditions under dClim 1.0 (year=2116); (F) future conditions under dClim 0.5 (year=2116).

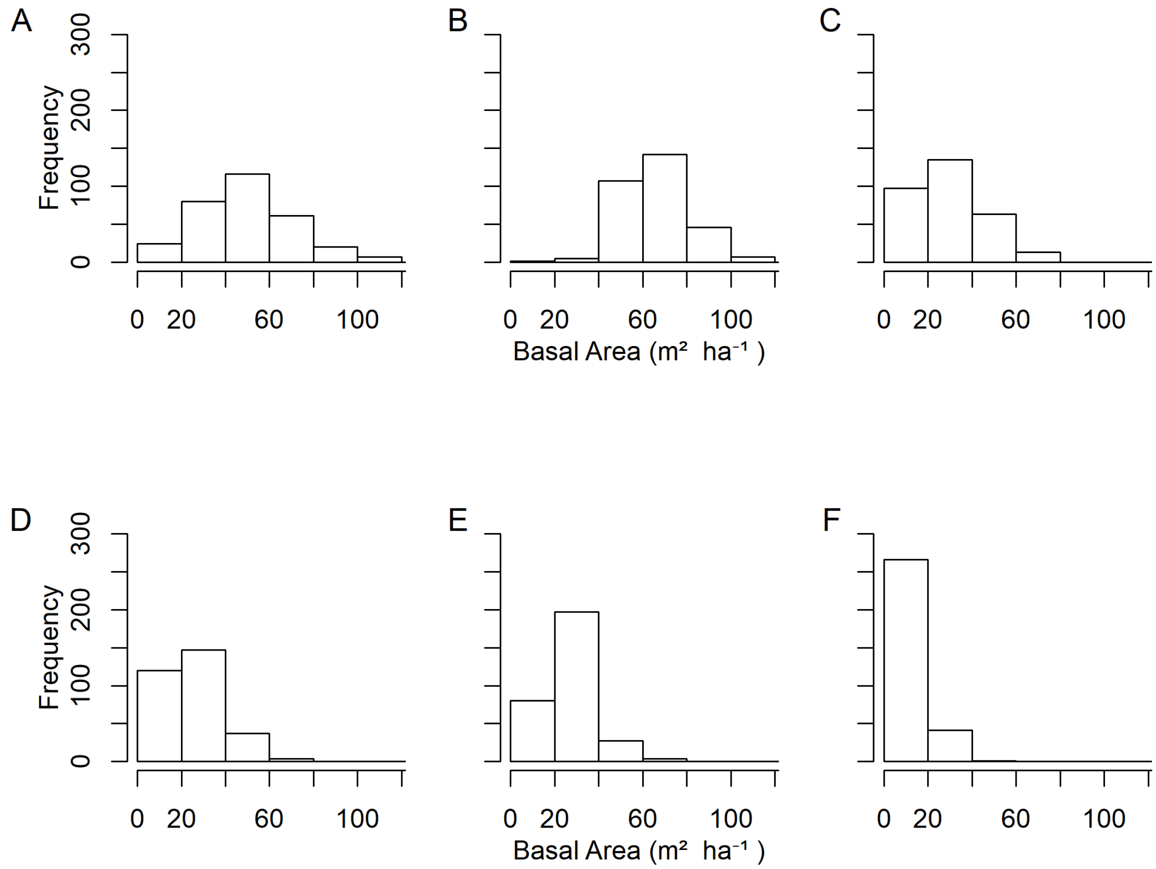

Figure S8: Siuslaw National Forest plot-level basal area distribution simulated using the base disturbance level for (A) current conditions (year=2016); (B) future conditions under no climate change (year=2116); (C) future conditions under dClim 2.0 (year=2116); (D) future conditions under dClim Off (year=2116); (E) future conditions under dClim 1.0 (year=2116); (F) future conditions under dClim 0.5 (year=2116).

References

1. Climate-FVS. Climate Estimates and Plant-Climate Relationships. 2019. Available from:

http://charcoal.cnre.vt.edu/climate/customData/fvs_data.php. Accessed 3 Mar 2019.